

Supporting information – Part 1 for the paper:

Computational Mutagenesis at the SARS-CoV-2 Spike Protein/Angiotensin-Converting Enzyme 2 Binding Interface: Comparison with Experimental Evidences

Erik Laurini^{1,‡}, Domenico Marson^{1,‡}, Suzana Aulic¹, Alice Fermeglia¹, Sabrina Prici^{1,2*}

¹Molecular Biology and Nanotechnology Laboratory (MolBNL@UniTS), DEA, University of Trieste, 34127 Trieste, Italy

²Department of General Biophysics, Faculty of Biology and Environmental Protection, University of Lodz, 90-136 Lodz, Poland

Table S1. Relative binding free energy and its components calculated by computational mutagenesis for the ACE2 residues effectively involved in the binding interface with the S-RBD of SARS-CoV-2 (see the SI Materials and Methods section for details). IE = interaction entropy. $\Delta\Delta G = \Delta G_{WT} - \Delta G_{MUT}$ (see text for details).

	Q24I	Q24S	Q24T	Q24D	Q24K	Q24W		T27I	T27S	T27T	T27D	T27K	T27W
$\Delta\Delta E_{DISP}$	-1.73	-1.81	0.57	-2.03	-2.19	-0.43	$\Delta\Delta E_{VDW}$	0.15	-0.11	-	0.62	0.04	0.47
$\Delta\Delta E_{ELE}$	-0.28	0.09	0.29	-0.92	-1.10	-1.21	$\Delta\Delta E_{ELE}$	-0.38	0.01	-	2.27	1.39	0.51
$\Delta\Delta H$	-2.01	-1.72	0.86	-2.95	-3.29	-1.64	$\Delta\Delta H$	-0.23	-0.10	-	2.89	1.43	0.98
$\Delta\Delta IE$	-0.02	-0.29	0.07	-0.28	-0.39	-0.04	$\Delta\Delta IE$	-0.18	0.02	-	0.22	0.09	0.04
$\Delta\Delta G_{ACE2}$	-2.03	-2.01	+0.93	-3.23	-3.68	-1.68	$\Delta\Delta G_{ACE2}$	-0.41	-0.08	-	3.11	1.52	1.02
	(0.14)	(0.09)	(0.05)	(0.17)	(0.11)	(0.09)		(0.13)	(0.11)	-	(0.09)	(0.16)	(0.14)
	F28I	F28S	F28T	F28D	F28K	F28W		D30I	D30S	D30T	D30E	D30K	D30W
$\Delta\Delta E_{DISP}$	-0.79	-1.12	-0.86	-0.99	-0.67	0.15	$\Delta\Delta E_{DISP}$	-0.81	-1.12	-0.84	0.65	-0.21	0.18
$\Delta\Delta E_{ELE}$	-0.02	-0.06	-0.05	-0.65	-1.01	-0.33	$\Delta\Delta E_{ELE}$	-2.22	-1.07	0.15	0.45	-3.40	-0.90
$\Delta\Delta H$	-0.81	-1.18	-0.91	-1.64	-1.68	-0.18	$\Delta\Delta H$	-3.03	-2.19	-0.69	1.10	-3.61	-0.72
$\Delta\Delta IE$	-0.01	-0.09	0.02	0.08	-0.15	-0.01	$\Delta\Delta IE$	-0.78	-0.65	-0.59	0.06	-0.9	-0.55
$\Delta\Delta G_{ACE2}$	-0.82	-1.27	-0.89	-1.56	-1.83	-0.19	$\Delta\Delta G_{ACE2}$	-3.81	-2.84	-1.28	1.16	-4.51	-1.27
	(0.17)	(0.16)	(0.14)	(0.11)	(0.18)	(0.13)		(0.15)	(0.06)	(0.10)	(0.17)	(0.18)	(0.11)
	K31I	K31S	K31T	K31D	K31R	K31W		H34I	H34S	H34T	H34D	H34K	H34W
$\Delta\Delta E_{DISP}$	-2.76	-2.52	-2.48	-2.83	0.22	0.76	$\Delta\Delta E_{DISP}$	-1.24	-0.19	-0.12	-0.30	1.02	-0.32
$\Delta\Delta E_{ELE}$	-2.70	-0.93	-1.02	-1.51	-0.84	-3.78	$\Delta\Delta E_{ELE}$	-0.55	0.79	0.66	-0.62	-0.58	-0.03
$\Delta\Delta H$	-5.46	-3.45	-3.50	-4.34	-0.62	-3.02	$\Delta\Delta H$	-1.79	0.60	0.54	-0.91	0.44	-0.35
$\Delta\Delta IE$	-0.15	-0.18	-0.22	-0.56	0.12	-0.05	$\Delta\Delta IE$	-0.32	0.12	0.11	-0.12	0.09	-0.19
$\Delta\Delta G_{ACE2}$	-5.61	-3.63	-3.72	-4.90	-0.50	-3.07	$\Delta\Delta G_{ACE2}$	-2.11	0.72	0.65	-1.03	0.53	-0.54
	(0.08)	(0.09)	(0.13)	(0.08)	(0.07)	(0.18)		(0.16)	(0.12)	(0.07)	(0.13)	(0.09)	(0.12)
	E35I	E35S	E35T	E35D	E35K	E35W		E37I	E37S	E37T	E37D	E37K	E37W
$\Delta\Delta E_{DISP}$	-1.01	-0.87	-1.07	0.03	0.15	0.79	$\Delta\Delta E_{DISP}$	-1.02	-1.97	-1.61	-0.82	-0.46	0.78
$\Delta\Delta E_{ELE}$	-3.17	-2.86	-2.85	0.83	-4.95	-5.20	$\Delta\Delta E_{ELE}$	-3.06	-2.73	-3.73	-2.99	-5.65	-3.55
$\Delta\Delta H$	-4.18	-3.73	-3.92	0.86	-4.80	-4.41	$\Delta\Delta H$	-4.08	-4.70	-5.34	-3.82	-6.11	-2.77
$\Delta\Delta IE$	-0.47	-0.37	-0.41	0.12	-0.28	-0.45	$\Delta\Delta IE$	-0.99	-0.84	-0.87	-0.78	-0.71	-0.75
$\Delta\Delta G_{ACE2}$	-4.65	-4.10	-4.33	0.98	-5.08	-4.86	$\Delta\Delta G_{ACE2}$	-5.07	-5.54	-6.21	-4.60	-6.82	-3.52
	(0.11)	(0.08)	(0.18)	(0.11)	(0.19)	(0.16)		(0.17)	(0.19)	(0.07)	(0.19)	(0.14)	(0.06)
	D38I	D38S	D38T	D38E	D38K	D38W		Y41I	Y41S	Y41T	Y41D	Y41K	Y41W
$\Delta\Delta E_{DISP}$	-1.78	-0.87	-1.01	-0.20	-1.98	-1.45	$\Delta\Delta E_{DISP}$	-1.10	-1.86	-1.16	-2.19	0.47	-0.78
$\Delta\Delta E_{ELE}$	-2.61	-2.94	-4.05	-0.07	-4.67	-4.40	$\Delta\Delta E_{ELE}$	-2.54	-0.90	-1.64	-2.63	-0.69	-1.32
$\Delta\Delta H$	-4.39	-3.81	-5.06	-0.27	-6.65	-5.85	$\Delta\Delta H$	-3.64	-2.76	-2.80	-4.82	-0.22	-2.10
$\Delta\Delta IE$	-1.09	-0.98	-1.26	-0.08	-1.24	-1.21	$\Delta\Delta IE$	-0.45	-0.48	-0.32	-0.31	0.04	-0.29
$\Delta\Delta G_{ACE2}$	-5.48	-4.79	-6.32	-0.35	-7.89	-7.06	$\Delta\Delta G_{ACE2}$	-4.09	-3.24	-3.12	-5.13	-0.18	-2.39
	(0.12)	(0.13)	(0.09)	(0.12)	(0.19)	(0.13)		(0.19)	(0.12)	(0.16)	(0.08)	(0.11)	(0.18)
	Q42I	Q42S	Q42T	Q42D	Q42K	Q42W		L79I	L79S	L79T	L79D	L79K	L79W
$\Delta\Delta E_{DISP}$	-0.78	-0.19	-0.12	-0.94	0.38	-0.36	$\Delta\Delta E_{DISP}$	0.32	-0.46	-0.28	-0.76	-0.26	0.67
$\Delta\Delta E_{ELE}$	-1.40	0.16	0.19	-1.32	-0.04	-1.01	$\Delta\Delta E_{ELE}$	0.04	0.45	0.36	0.12	0.30	0.33
$\Delta\Delta H$	-2.18	-0.03	0.07	-2.27	0.34	-1.37	$\Delta\Delta H$	0.36	-0.01	0.08	-0.64	0.04	1.00
$\Delta\Delta IE$	-0.28	-0.05	0.03	-0.45	0.11	-0.42	$\Delta\Delta IE$	-0.01	-0.03	0.02	-0.27	-0.22	0.05
$\Delta\Delta G_{ACE2}$	-2.46	-0.08	0.10	-2.72	0.45	-1.79	$\Delta\Delta G_{ACE2}$	0.35	-0.04	0.10	-0.91	-0.18	1.05
	(0.10)	(0.06)	(0.11)	(0.18)	(0.07)	(0.19)		(0.10)	(0.14)	(0.16)	(0.19)	(0.06)	(0.15)
	M82I	M82S	M82T	M82D	M82K	M82W		Y83I	Y83S	Y83T	Y83D	Y83K	Y83W
$\Delta\Delta E_{DISP}$	0.03	-0.59	-0.47	-0.86	0.15	0.26	$\Delta\Delta E_{DISP}$	-1.52	-2.35	-2.39	-1.89	-2.65	-0.37
$\Delta\Delta E_{ELE}$	-0.14	-0.03	-0.23	0.57	-0.12	-0.36	$\Delta\Delta E_{ELE}$	-1.18	-0.51	-0.78	-0.30	-0.67	-0.53
$\Delta\Delta H$	-0.11	-0.62	-0.70	-0.29	0.03	-0.10	$\Delta\Delta H$	-1.70	-2.86	-3.17	-2.19	-3.32	-0.90
$\Delta\Delta IE$	-0.02	-0.05	-0.04	-0.14	0.04	0.01	$\Delta\Delta IE$	-0.28	-0.18	-0.16	-0.18	-0.26	-0.11
$\Delta\Delta G_{ACE2}$	-0.13	-0.67	-0.74	-0.43	0.07	-0.09	$\Delta\Delta G_{ACE2}$	-2.98	-3.04	-3.33	-2.37	-3.58	-1.01
	(0.05)	(0.07)	(0.14)	(0.16)	(0.15)	(0.11)		(0.19)	(0.06)	(0.16)	(0.17)	(0.11)	(0.18)

	K353I	K353S	K353T	K353D	K353R	K353W		D355I	D355S	D355T	D355E	D355K	D355W
$\Delta\Delta E_{DISP}$	-0.72	-2.45	-1.98	-4.31	-1.05	-2.98	$\Delta\Delta E_{DISP}$	-3.29	-2.71	-2.54	0.02	-1.75	-1.01
$\Delta\Delta E_{ELE}$	-4.75	-3.47	-3.11	-2.07	-0.31	-4.56	$\Delta\Delta E_{ELE}$	-4.21	0.05	0.35	-0.06	-3.47	-2.25
$\Delta\Delta H$	-5.47	-5.92	-5.09	-6.38	-1.36	-7.54	$\Delta\Delta H$	-7.50	-2.66	-2.19	-0.04	-5.22	-3.26
$\Delta\Delta IE$	-1.2	-1.02	-0.95	-1.87	-0.07	-1.99	$\Delta\Delta IE$	-0.87	-0.56	-0.48	-0.02	-1.19	-0.73
$\Delta\Delta G_{ACE2}$	-6.67	-6.94	-6.04	-8.25	-1.43	-9.53	$\Delta\Delta G_{ACE2}$	-8.37	-3.22	-2.67	-0.06	-6.41	-3.99
	(0.08)	(0.06)	(0.09)	(0.10)	(0.12)	(0.15)		(0.15)	(0.16)	(0.10)	(0.11)	(0.08)	(0.07)
	R357I	R357S	R357T	R357D	R357K	R357W		R393I	R393S	R393T	R393D	R393K	R393W
$\Delta\Delta E_{DISP}$	-1.47	-2.03	-1.52	-1.16	-0.05	-0.74	$\Delta\Delta E_{DISP}$	-0.94	-0.43	-0.36	-0.39	0.30	-0.35
$\Delta\Delta E_{ELE}$	-1.96	-2.38	-2.68	-2.83	0.95	-1.56	$\Delta\Delta E_{ELE}$	-1.25	-1.45	-1.34	-3.19	0.45	-0.81
$\Delta\Delta H$	-3.43	-4.41	-4.20	-3.99	0.90	-2.30	$\Delta\Delta H$	-2.19	-1.88	-1.70	-3.58	0.75	-1.16
$\Delta\Delta IE$	-0.59	-0.67	-0.57	-0.38	0.03	-0.16	$\Delta\Delta IE$	-0.39	-0.27	-0.28	-0.47	0.04	-0.41
$\Delta\Delta G_{ACE2}$	-4.02	-5.08	-4.77	-4.37	0.93	-2.46	$\Delta\Delta G_{ACE2}$	-2.58	-2.15	-1.98	-4.05	0.79	-1.57
	(0.15)	(0.10)	(0.19)	(0.05)	(0.11)	(0.09)		(0.17)	(0.19)	(0.08)	(0.12)	(0.14)	(0.09)

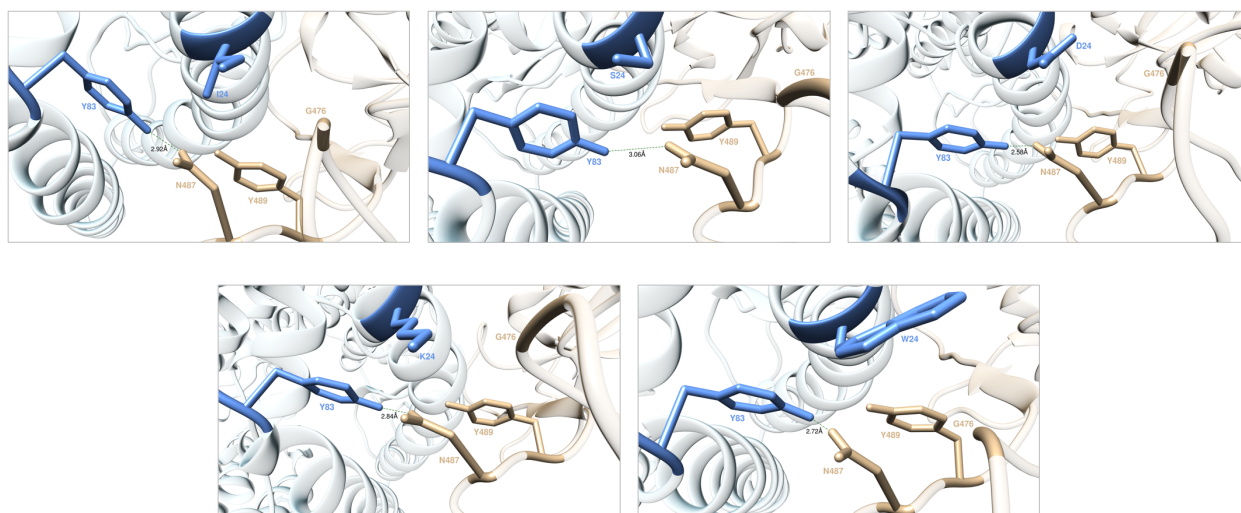


Figure S1. Main interactions involving the ACE2 I24 (top left), S24 (top middle), D24 (top right), K24 (bottom left), and W24 (bottom right) at the interface with S-RBD_{CoV-2} as obtained from the corresponding equilibrated MD simulations. The wild-type Q24 and the T24 mutant are presented and discussed in the main text (Figure 2A-B). In this and all remaining Figures, the secondary structures of ACE2 and S-RBD_{CoV-2} are portrayed as light blue and light sienna ribbons, respectively. Each protein residue under discussion and all other residues directly interacting with them are highlighted in dark matching-colored sticks and labelled; further residues/interactions related to the residue under investigation are evidenced in light matching-colored sticks and labelled in light gray. Hydrogen bonds and salt bridges are represented as dark green and dark red broken lines, respectively, and the relevant average distances are reported (in black) accordingly; new HBs and SBs detected in each mutant complex are also indicated using dark green/red broken lines and black labels. For further details see Tables S1 and S3.

Table S3. Main intermolecular and intramolecular interactions between the wild-type ACE2 residue Q24 and all considered mutants* at the protein-protein interface detected during MD simulations of ACE2 in complex with the RBD of SARS-CoV-2 (COV-2). HB = hydrogen bond; SB = salt bridge; CI = contact interactions, including van der Waals/hydrophobic (vdW/h), polar (p), π/π and π /cation (π/c) interactions. In the HB column, s-s indicates side chain-side chain interactions while s-b (or b-s) and b-b indicate side chain-backbone and backbone-backbone interactions, respectively. Preserved/new or lost interactions are marked with the symbols \checkmark and \times , respectively. Relevant changes in the type/nature of the interactions are indicated in parenthesis. For HBs and SBs, the relevant average lengths (in Å) are also reported (their standard deviations, all within 10%, are not shown for clarity). Charges not involved in SBs at the protein/protein interface are also indicated. *Mutant T24 is discussed in detail in main text.

HB	COV-2	ACE2	Q24	I24	S24	T24	D24	K24	W24
s-s	N487	X24	\checkmark (3.03)	\times	\times	\checkmark (3.13)	\times	\times (p)	\times
s-s	N487	Y83	\checkmark (2.88)	\checkmark (2.92)	\checkmark (3.06)	\checkmark (2.73)	\checkmark (2.58)	\checkmark (2.84)	\checkmark (2.72)
HB	ACE2	ACE2	Q24	I24	S24	T24	D24	K24	W24
s-s	Y83	X24	\times	\times	\times	\checkmark (3.45)	\times	\times	\times
CI	COV-2	ACE2	Q24	I24	S24	T24	D24	K24	W24
vdW/h	G476	X24	\checkmark	\times	\times	\checkmark	\checkmark	\times	\times
vdW/h	Y489	X24	\checkmark	\checkmark	\checkmark (p)	\checkmark (p)	\times	\times	\checkmark
vdW/h	Y83	X24	\checkmark	\times	\times	\checkmark	\times	\checkmark (p)	\times

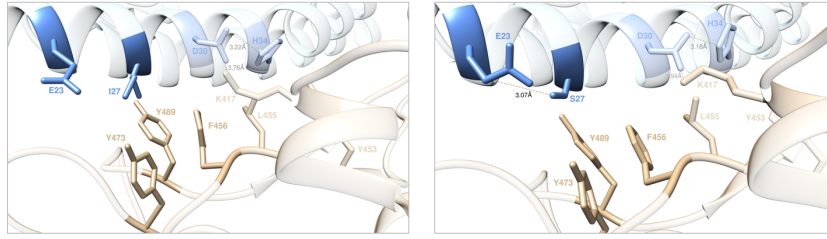


Figure S2. Main interactions involving the ACE2 I27 (left) and S27 (right) at the interface with S-RBD_{CoV-2} as obtained from the corresponding equilibrated MD simulations. The wild-type residue T27 and the D27, K27, and W27 mutants are presented and discussed in the main text (Figure 2C-F). Colors and other explanations as in Figure S1. For further details see Tables S1 and S4.

Table S4. Main intermolecular and intramolecular interactions between the wild-type ACE2 residue T27 and all considered mutants* at the protein-protein interface detected during MD simulations of ACE2 in complex with the RBD of SARS-CoV-2 (COV-2). Acronyms and other explanations as in Table S3. *Mutants D27, K27 and W27 are discussed in detail in main text.

HB	COV-2	ACE2	T27	I27	S27	D27	K27	W27
s-s	Y473	X27	X	X	X	✓(2.68)	X	X
s-s	Y453	H34	X(p)	X(p)	X(p)	✓(3.37)	✓(3.24)	✓(3.48)
HB	ACE2	ACE2	T27	I27	S27	D27	K27	W27
b-s	E23	X27	✓(3.05)	X	✓(3.07)	X	✓(SB,3.74)	X
s-s	D30	H34	✓(3.31)	✓(3.22)	✓(3.18)	✓(2.90)	✓(3.04)	✓(3.37)
SB	COV-2	ACE2	T27	I27	S27	D27	K27	W27
	K417	X27	X	X	X	✓(3.87)	X	X
	K417	D30	✓(3.85)	✓(3.76)	✓(3.94)	✓(3.67)	✓(3.84)	✓(3.91)
CI	COV-2	ACE2	T27	I27	S27	D27	K27	W27
vdW/h	F456	X27	✓	✓	✓	✓	✓	✓(π/π)
vdW/h	Y489	X27	✓	✓	✓	✓	✓	✓
vdW/h	Y473	X27	✓	✓	✓	✓	✓	✓

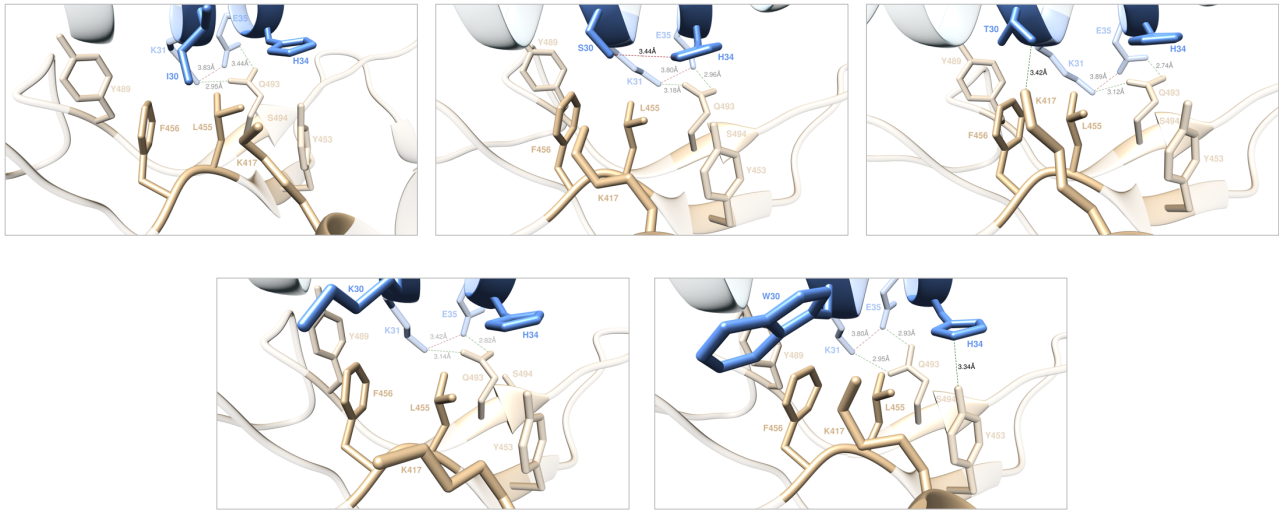


Figure S3. Main interactions involving the ACE2 I30 (top left), S30 (top middle), T30 (top right), K30 (bottom left) and W30 (bottom right) at the interface with S-RBD_{CoV-2} as obtained from the corresponding equilibrated MD simulations. The wild-type D30 and the E30 mutant are presented and discussed in the main text (Figure 4A-B). Colors and other explanations as in Figure S1. For further details see Tables S1 and S5.

Table S5. Main intermolecular and intramolecular interactions between the wild-type ACE2 residue D30 and all considered mutants* at the protein-protein interface detected during MD simulations of ACE2 in complex with the RBD of SARS-CoV-2 (CoV-2). Acronyms and other explanations as in Table S3. *Mutant E30 is discussed in detail in main text.

HB	COV-2	ACE2	D30	I30	S30	T30	E30	K30	W30
s-s	Q493	K31	✓(3.04)	✓(2.95)	✓(3.18)	✓(3.12)	✓(2.85)	✓(3.14)	✓(2.95)
s-s	Q493	E35	✓(2.94)	✓(3.44)	✓(2.96)	✓(2.74)	✓(3.31)	✓(2.82)	✓(2.93)
HB	ACE2	ACE2	D30	I30	S30	T30	E30	K30	W30
s-s	H34	X30	✓(3.31)	✗	✓(3.44)	✗	✓(2.96)	✗	✗
HB	COV2	COV2	D30	I30	S30	T30	E30	K30	W30
s-s	Q493	S494	✓(3.24)	✗	✗	✗	✗	✗	✗
SB	COV-2	ACE2	D30	I30	S30	T30	E30	K30	W30
	K417	X30	✓(3.85)	✗	✗	✓(HB,3.42)	✓(3.01)	✗	✗
SB	ACE2	ACE2	D30	I30	S30	T30	E30	K30	W30
	K31	E35	✓(3.94)	✓(3.83)	✓(3.80)	✓(3.89)	✓(3.08)	✓(3.42)	✓(3.80)
CI	COV-2	ACE2	D30	I30	S30	T30	E30	K30	W30
vdW/h	F456	X30	✓	✓	✓	✓	✓	✓	✗
vdW/h	L455	X30	✓	✓	✓	✓	✓	✗	✗
p	Y453	H34	✓	✓	✓	✓	✓	✓	✓(HB,3.34)
vdw/h	Y489	K31	✓	✓	✓	✓	✓	✓	✓

The qualitative *in silico*/experimental data comparison shown in Figure 5A (main text) for the mutagenesis of ACE D30 into the 6 residues considered it appears that the only different trend concerns mutation I30, for which a slightly beneficial effect is reported by experiment while an interface disrupting effect is predicted ($\Delta\Delta G_{ACE2}(D30I) = -3.81 \pm 0.15$ kcal/mol, Table S1). The analysis of the corresponding MD trajectory for the ACE2 I30 mutant in complex with the S-RBD_{CoV-2} (Figure S3 (top left) and Table S5) reveals that, with respect to the wild-type assembly, three important interface interactions are no longer detected in the presence of the hydrophobic mutant residue: i) the intramolecular HB between the side chains of D30 and H34 on ACE2; ii) the intramolecular Q493-S494 HB on S-RBD_{CoV-2}, and iii) the intermolecular, charge-neutralizing SB between D30 on ACE2 and K417 on the viral protein. According to Shang *et al.*¹,

neutralizing the charges of the lysines is a key factor in the binding of coronavirus RBDs to ACE2. Moreover, as reported by Lan *et al.*² and verified in our previous work,³ K417 is the only residue on the S-RBD_{CoV-2} able to form an intermolecular SB with ACE D30 (Figure 4A, main text). Interestingly, in the receptor binding site of SARS-CoV K417 is replaced by V404, and this residue fails to participate in ACE2 binding.² Finally, in the experimental ACE deep mutagenesis study reported by Chan *et al.*⁴ similar substitutions at ACE position 30 – *i.e.*, D30M, D30L and D30A – are also reported to be interface disrupting mutations. Accordingly, we retain that a charged-to-hydrophobic substitution at this receptor position ultimately exerts destabilizing effects on the ACE2/S-RBD_{CoV-2} complex formation.

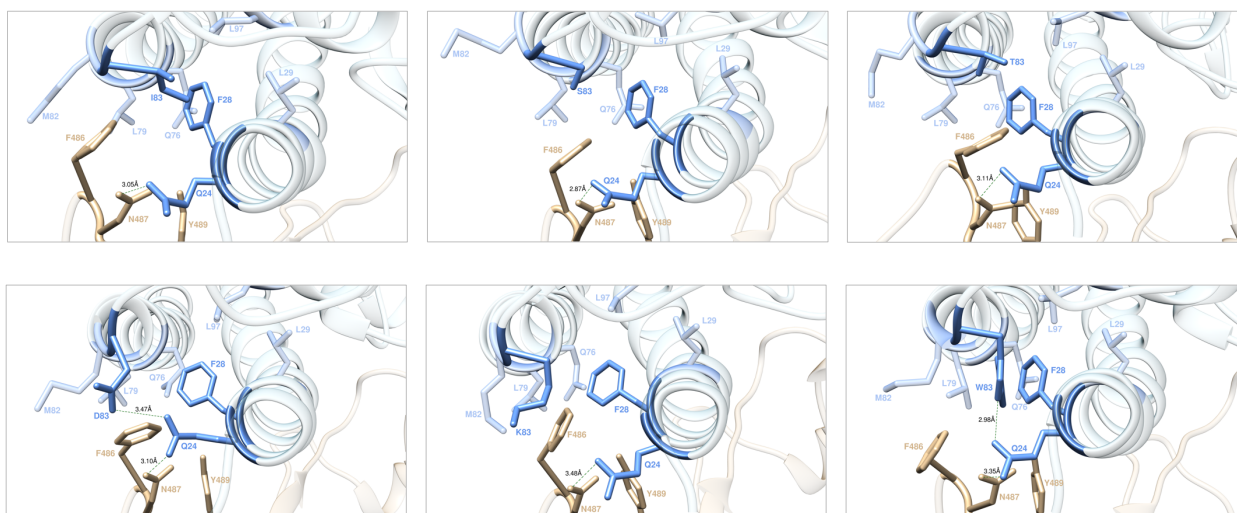


Figure S5. Main interactions involving the ACE2 I83 (top left), S83 (top middle), T83 (top right), D83 (bottom left), K83 (bottom middle) and W83 (bottom right) at the interface with S-RBD_{CoV-2} as obtained from the corresponding equilibrated MD simulations. The wild-type Y83 is presented and discussed in the main text (Figure 6A). Colors and other explanations as in Figure S1. For further details see Tables S1 and S7.

Table S7. Main intermolecular and intramolecular interactions between the wild-type ACE2 residue Y83 and all considered mutants at the protein-protein interface detected during MD simulations of ACE2 in complex with the RBD of SARS-CoV-2 (CoV-2). Acronyms and other explanations as in Table S3.

HB	COV-2	ACE2	Y83	I83	S83	T83	D83	K83	W83
s-s	N487	X83	✓(2.88)	✗	✗	✗	✗	✗	✗
s-s	N487	Q24	✓(3.03)	✓(3.05)	✓(2.87)	✓(3.11)	✓(3.10)	✓(3.48)	✓(3.35)
HB	ACE2	ACE2	Y83	I83	S83	T83	D83	K83	W83
s-s	Q24	X83	✗	✗	✗	✗	✓(3.47)	✗	✓(2.98)
CI	COV-2	ACE2	Y83	I83	S83	T83	D83	K83	W83
vdW/h	F486	X83	✓	✗	✗	✗	✓	✓	✗
p	Y489	X83	✓	✗	✗	✗	✗	✗	✗
CI	ACE2	ACE2	Y83	I83	S83	T83	D83	K83	W83
vdW/h	F28	X83	✓	✓	✓	✓	✗	✓	✓

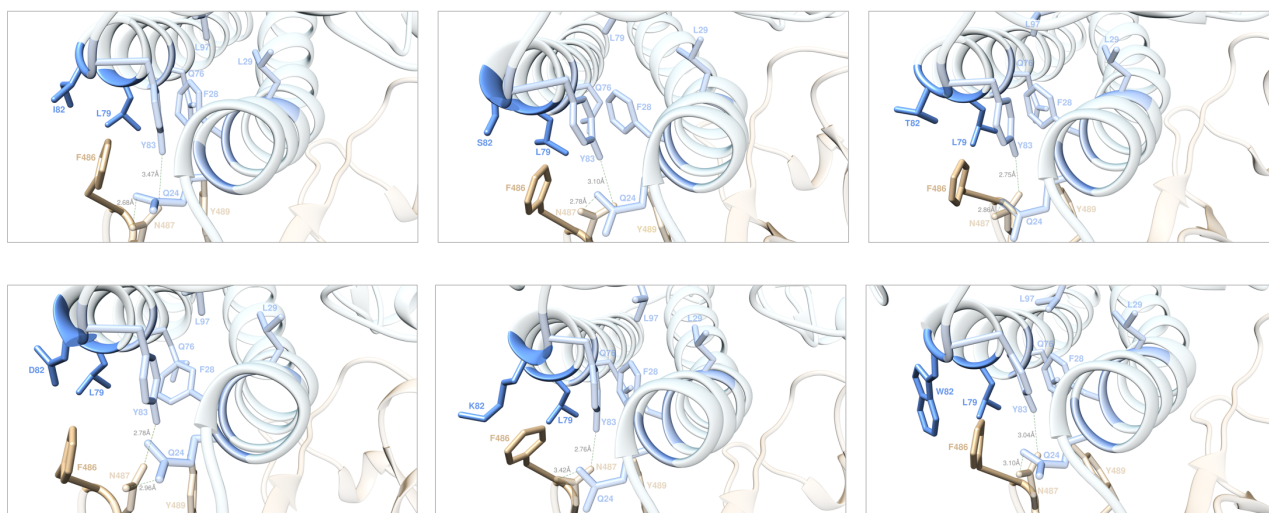


Figure S6. Main interactions involving the ACE2 I82 (top left), S82 (top middle), T82 (top right), D82 (bottom left), K82 (bottom middle) and W82 (bottom right) at the interface with S-RBD_{CoV-2} as obtained from the corresponding equilibrated MD simulations. The wild-type M82 is presented and discussed in the main text (Figure 6A). Colors and other explanations as in Figure S1. For further details see Tables S1 and S8.

Table S8. Main intermolecular and intramolecular interactions between the wild-type ACE2 residue M82 and all considered mutants at the protein-protein interface detected during MD simulations of ACE2 in complex with the RBD of SARS-CoV-2 (COV-2). Acronyms and other explanations as in Table S3.

HB	COV-2	ACE2	M82	I82	S82	T82	D82	K82	W82
s-s	N487	Y83	✓(2.88)	✓(3.47)	✓(3.10)	✓(2.75)	✓(2.78)	✓(2.76)	✓(3.04)
s-s	N487	Q24	✓(3.03)	✓(2.68)	✓(2.78)	✓(2.86)	✓(2.96)	✓(3.42)	✓(3.10)
CI	COV-2	ACE2	M82	I82	S82	T82	D82	K82	W82
vdW/h	F486	X82	✓	✓	✗	✗	✓	✓	✓
vdw/h	F486	L79	✓	✓	✓	✓	✗	✓	✓
vdW/h	F486	Y83	✓	✓	✓	✗	✗	✓	✓
p	Y489	Y83	✓	✓	✓	✓	✓	✓	✓
CI	ACE2	ACE2	M82	I82	S82	T82	D82	K82	W82
vdW/h	L79	X82	✓	✓	✗	✗	✓	✓	✓
vdW/h	F28	L79	✓	✓	✗	✗	✓	✓	✓

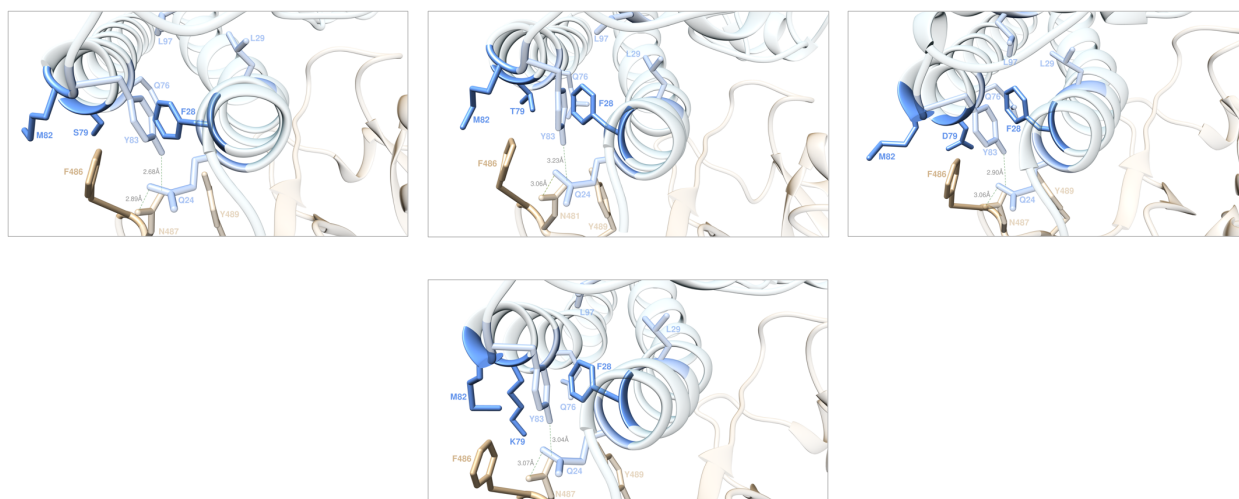


Figure S7. Main interactions involving the ACE2 S79 (top left), T79 (top middle), D79 (top right), and K79 (bottom), at the interface with S-RBD_{CoV-2} as obtained from the corresponding equilibrated MD simulations. The wild-type L79 and the mutants I79 and W79 are presented and discussed in the main text (Figure 6A-C). Colors and other explanations as in Figure S1. For further details see Tables S1 and S9.

Table S9. Main intermolecular and intramolecular interactions between the wild-type ACE2 residue L79 and all considered mutants* at the protein-protein interface detected during MD simulations of ACE2 in complex with the RBD of SARS-CoV-2 (COV-2). Acronyms and other explanations as in Table S3. *Mutants I79 and W79 are discussed in detail in main text.

HB	COV-2	ACE2	L79	I79	S79	T79	D79	K79	W79
s-s	N487	Y83	✓(2.88)	✓(2.80)	✓(2.68)	✓(3.23)	✓(2.90)	✓(3.04)	✓(2.69)
s-s	N487	Q24	✓(3.03)	✓(2.99)	✓(2.89)	✓(3.06)	✓(3.06)	✓(3.07)	✓(3.01)
CI	COV-2	ACE2	L79	I79	S79	T79	D79	K79	W79
vdw/h	F486	X79	✓	✓	✓	✓	✓	✓	✓(π/π)
vdW/h	F486	M82	✓	✓	✓	✓	✗	✓	✓
p	Y489	Y83	✓	✓	✓	✓	✓	✓	✓
CI	ACE2	ACE2	L79	I79	S79	T79	D79	K79	W79
vdW/h	M82	X79	✓	✓	✓	✓	✗	✓	✓
vdW/h	F28	X79	✓	✓	✓	✓	✗	✓	✓
vdW/h	F28	Y83	✓	✓	✓	✓	✓	✓	✓

As it can be inferred by comparing the top left and middle panels in Figure S7 and the data listed in Table S9, according to our MD simulations the two ACE2 mutants S79 and T79 both establish the same interaction network seen from the wild-type protein (Figure 6A in main text). The small difference resides only in the somewhat longer length of the two intermolecular HBs involving Y83 and Q24 on ACE2 and N487 on the S-protein in the case of the L79T mutant complex. In agreement with this, the relevant $\Delta\Delta G$ values are therefore very small and comparable ($\Delta\Delta G_{ACE2}(L79S) = -0.04 \pm 0.14$ kcal/mol and $\Delta\Delta G_{ACE2}(L79T) = -0.10 \pm 0.16$ kcal/mol, respectively, Figure 7C and Table S1), supporting a neutral effect for both these ACE2 substitutions on the affinity for the viral protein.

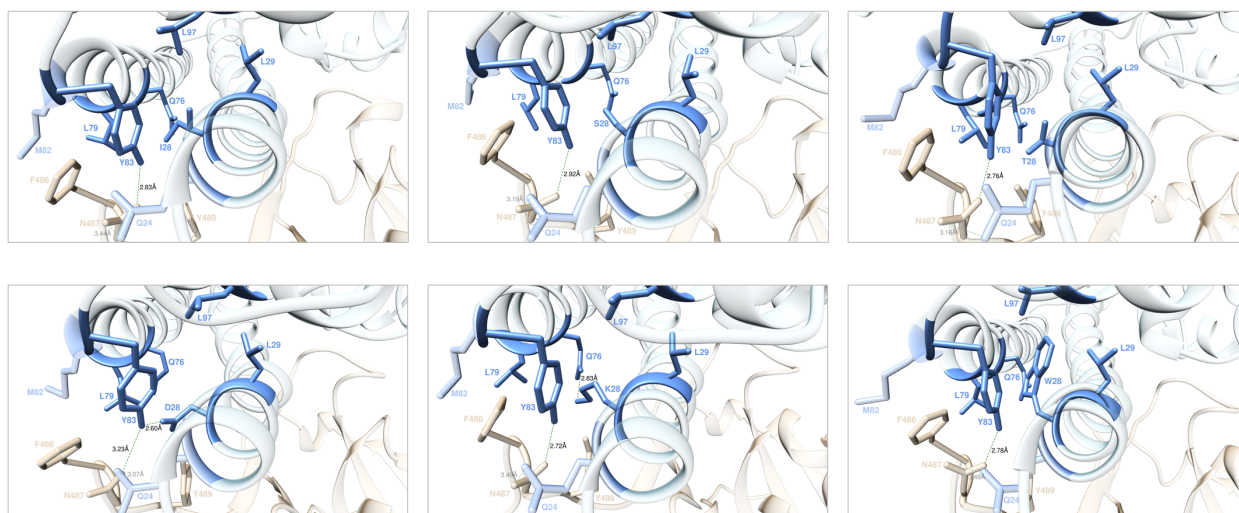


Figure S8. Main interactions involving the ACE2 I28 (top left), S28 (top middle), T28 (top right), D28 (bottom left), K28 (bottom middle) and W28 (bottom right) at the interface with S-RBD_{CoV-2} as obtained from the corresponding equilibrated MD simulations. The wild-type F82 is presented and discussed in the main text (Figure 6A). Colors and other explanations as in Figure S1. For further details see Tables S1 and S10.

Table S10. Main intermolecular and intramolecular interactions between the wild-type ACE2 residue F28 and all considered mutants at the protein-protein interface detected during MD simulations of ACE2 in complex with the RBD of SARS-CoV-2 (COV-2). Acronyms and other explanations as in Table S3.

HB	COV-2	ACE2	F28	I28	S28	T28	D28	K28	W28
s-s	N487	Y83	✓(2.88)	✓(2.83)	✓(2.92)	✓(2.76)	✓(3.23)	✓(2.72)	✓(2.78)
s-s	N487	Q24	✓(3.03)	✓(3.44)	✓(3.19)	✓(3.16)	✓(3.07)	✓(3.49)	✓(3.48)
CI	COV-2	ACE2	F28	I28	S28	T28	D28	K28	W28
vdw/h	F486	L79	✓	✗	✗	✓	✗	✓	✓
p	Y489	Y83	✓	✓	✓	✓	✗	✗	✗
CI	ACE2	ACE2	F28	I28	S28	T28	D28	K28	W28
vdW/h	L29	X28	✓	✗	✗	✗	✗	✗	✓
vdW/h	Q76	X28	✓	✓	✓	✓	✗	✓(HB,2.83)	✓
vdW/h	Y83	X28	✓	✓	✓	✓	✓(HB,2.60)	✗	✓
vdW/h	L79	X28	✓	✗	✗	✗	✓	✗	✗
vdW/h	L97	X28	✓	✗	✗	✗	✗	✗	✓

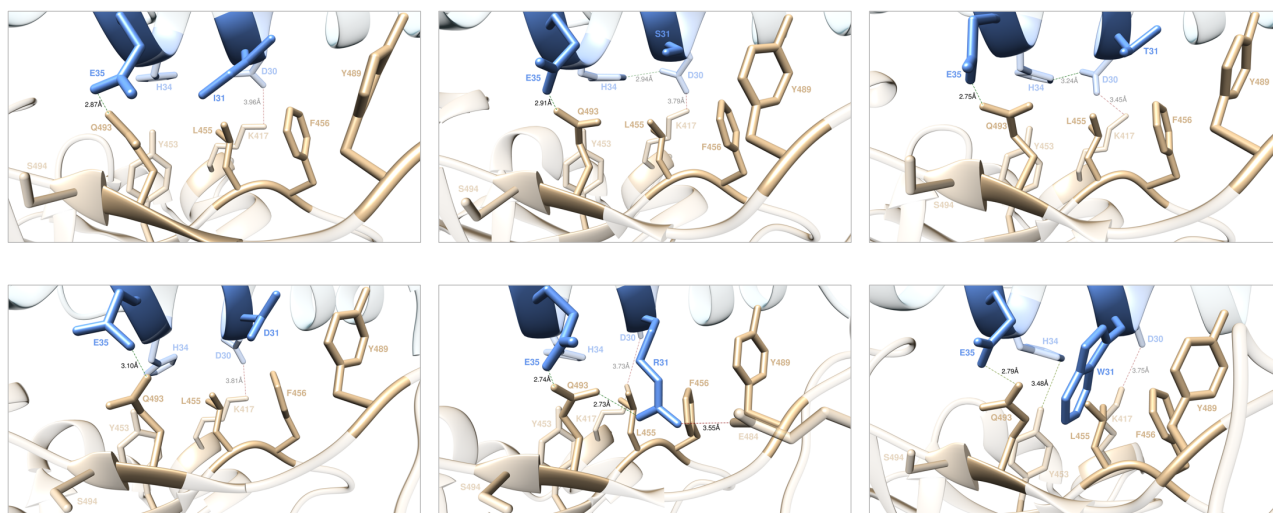


Figure S9. Main interactions involving the ACE2 I31 (top left), S31 (top middle), T31 (top right), D31 (bottom left), R31 (bottom middle) and W31 (bottom right) at the interface with S-RBD_{Cov-2} as obtained from the corresponding equilibrated MD simulations. The wild-type K31 is presented and discussed in the main text (Figure 8A). Colors and other explanations as in Figure S1. For further details see Tables S1 and S11.

Table S11. Main intermolecular and intramolecular interactions between the wild-type ACE2 residue K31 and all considered mutants at the protein-protein interface detected during MD simulations of ACE2 in complex with the RBD of SARS-CoV-2 (COV-2). Acronyms and other explanations as in Table S3.

HB	COV-2	ACE2	K31	I31	S31	T31	D31	R31	W31
s-s	Q493	X31	✓(3.04)	✗	✗	✗	✗	✓(2.73)	✗
s-s	Q493	E35	✓(2.94)	✓(2.87)	✓(2.91)	✓(2.75)	✓(3.10)	✓(2.74)	✓(2.79)
SB	ACE2	ACE2	K31	I31	S31	T31	D31	R31	W31
	E35	X31	✓(3.94)	✗	✗	✗	✗	✗	✗
HB	COV-2	COV-2	K31	I31	S31	T31	D31	R31	W31
s-s	Q493	S494	✓(3.24)	✗	✗	✗	✗	✗	✗
SB	COV-2	ACE2	K31	I31	S31	T31	D31	R31	W31
	E484	X31	✗	✗	✗	✗	✗	✓(3.55)	✗
	K417	D30	✓(3.85)	✓(3.96)	✓(3.79)	✓(3.45)	✓(3.81)	✓(3.73)	✓(3.75)
HB	ACE2	ACE2	K31	I31	S31	T31	D31	R31	W31
s-s	H34	D30	✓(3.31)	✗	✓(2.94)	✓(3.24)	✗	✗	✗
CI	COV-2	ACE2	K31	I31	S31	T31	D31	R31	W31
vdw/h	Y489	X31	✓	✓	✗	✓	✓	✓	✓
vdW/h	L455	X31	✓	✓	✓	✓	✓	✓	✓
vdW/h	F456	X31	✓	✓	✓	✓	✓	✓	✓
vdW/h	F456	D30	✓	✓	✓	✓	✓	✗	✓
vdW/h	L455	D30	✓	✗	✓	✗	✗	✓	✗
p	Y453	H34	✓	✓	✓	✓	✓	✓	✓(HB,3.48)

According to the experimental study by Chan *et al.*,⁴ the substitution of the long, positively-charged K31 residue with the bulky and hydrophobic tryptophan results in a positive (*i.e.*, stabilizing) effect the corresponding protein/protein interface. On the other hand, our simulations predict that, when W replaces the native K at the same position, the affinity of the mutant receptor for the viral S-protein decreases ($\Delta\Delta G_{ACE2}(K31W) = -3.07 \pm 0.18$ kcal/mol, Figure 9A and

Table S1). The main reasons for this loss in binding free energy can be rationalized on the basis of the following major missing interactions at the relative W31 mutant ACE2/S-RBD_{CoV-2} interface: i) the charge-neutralizing ACE2 intramolecular SB between K31 and E35, ii) the intermolecular HB between K31 and the viral residue Q493; iii) the S-protein RBD internal HB between Q493 and S494, and iv) the structurally important intramolecular ACE2 HB between D30 and H34 (Table S11). These MD-based evidences along with the importance of lysine charge switch-off in the formation of the ACE2/S-RBD_{CoV-2} complex¹ in our opinion support the negative effect of the K31W ACE2 mutation at the human receptor/viral protein interface.

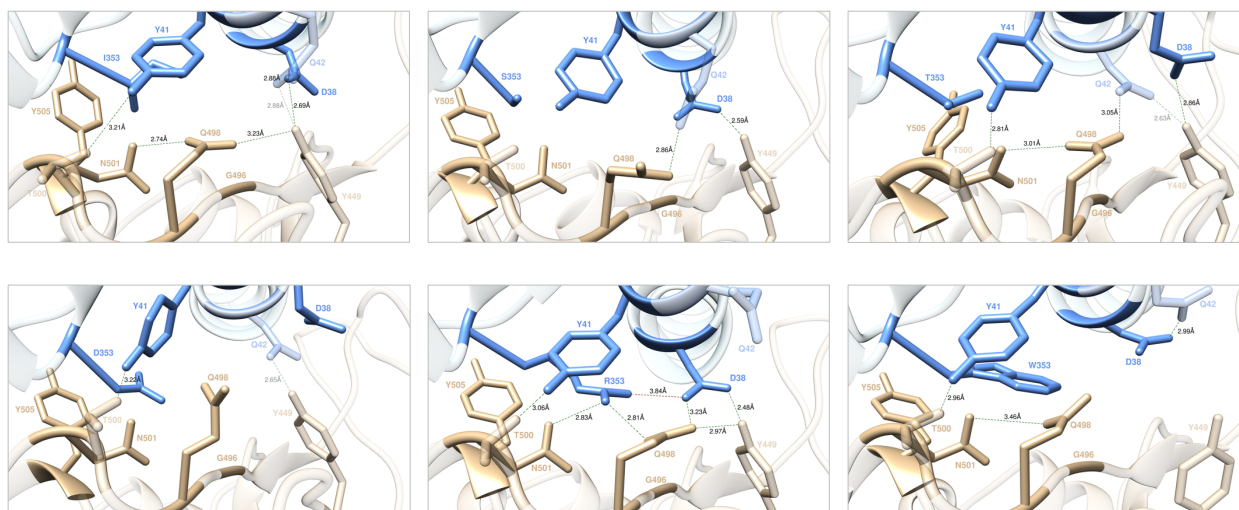


Figure S11. Main interactions involving the ACE2 I353 (top left), S353 (top middle), T353 (top right), D353 (bottom left), R353 (bottom middle) and W353 (bottom right) at the interface with S-RBD_{CoV-2} as obtained from the corresponding equilibrated MD simulations. The wild-type K353 is presented and discussed in the main text (Figure 10A). Colors and other explanations as in Figure S1. For further details see Tables S1 and S13.

Table S13. Main intermolecular and intramolecular interactions between the wild-type ACE2 residue K353 and all considered mutants at the protein-protein interface detected during MD simulations of ACE2 in complex with the RBD of SARS-CoV-2 (COV-2). Acronyms and other explanations as in Table S3.

HB	COV-2	ACE2	K353	I353	S353	T353	D353	R353	W353
s-s	Q498	X353	✓(2.87)	✗	✗	✗	✗	✓(2.81)	✗
b-s	G496	X353	✓(2.95)	✗	✗	✗	✗	✗	✗
s-s	T500	Y41	✓(3.08)	✓(3.21)	✗(p)	✓(2.81)	✓(3.22)	✓(3.06)	✓(2.96)
s-s	N501	Y41	✓(3.23)	✗	✗(p)	✗(p)	✗	✗(p)	✗(p)
s-s	Q498	D38	✓(2.92)	✗	✗	✗	✗	✓(3.23)	✗
s-s	N501	X353	✗(p)	✗(p)	✗(p)	✗	✗(p)	✓(2.83)	✗(p)
s-s	Y449	D38	✓(2.92)	✓(2.69)	✓(2.59)	✓(2.86)	✗	✓(2.48)	✗
s-s	Y449	Q42	✓(3.03)	✓(2.88)	✗	✓(2.63)	✓(2.65)	✗	✗
s-s	Q498	Q42	✗	✗	✓(2.86)	✓(3.05)	✗	✗	✗
SB	ACE2	ACE2	K353	I353	S353	T353	D353	R353	W353
	D38	X353	✓(3.66)	✗	✗	✗	✗	✓(3.84)	✗
HB	ACE2	ACE2	K353	I353	S353	T353	D353	R353	W353
b-s	D38	Q42	✓(3.04)	✓(s-s,2.88)	✗	✗	✗(p)	✗	✓(2.99)
HB	COV-2	COV-2	K353	I353	S353	T353	D353	R353	W353
s-s	N501	Q498	✓(3.02)	✓(2.74)	✗	✓(3.01)	✗	✗	✓(3.46)
s-s	Y449	Q498	✓(3.04)	✓(3.23)	✗	✗	✗	✓(2.97)	✗
CI	COV-2	ACE2	K353	I353	S353	T353	D353	R353	W353
vdW/h	Y505	X353	✓	✓	✓	✓	✓	✓	✓
p	Q498	Q42	✓	✗	✓	✓	✓	✗	✗
CI	ACE2	ACE2	K353	I353	S353	T353	D353	R353	W353
vdW/h	Y41	X353	✓	✓	✓(p)	✓(p)	✓	✓	✓



Figure S12. Main interactions involving the ACE2 I38 (top left), S38 (top middle), T38 (top right), E38 (bottom left), K38 (bottom middle) and W38 (bottom right) at the interface with S-RBD_{CoV-2} as obtained from the corresponding equilibrated MD simulation s. The wild-type D38 is presented and discussed in the main text (Figure 10A). Colors and other explanations as in Figure S1. For further details see Tables S1 and S14.

Table S14. Main intermolecular and intramolecular interactions between the wild-type ACE2 residue D38 and all considered mutants at the protein-protein interface detected during MD simulations of ACE2 in complex with the RBD of SARS-CoV-2 (COV-2). Acronyms and other explanations as in Table S3.

HB	COV-2	ACE2	D38	I38	S38	T38	E38	K38	W38
s-s	Q498	K353	✓(2.87)	✓(2.69)	✓(2.80)	✓(3.49)	✓(2.72)	X	X
b-s	G496	K353	✓(2.95)	✓(2.78)	✓(2.81)	✓(2.97)	✓(2.91)	✓(2.86)	✓(2.77)
s-s	T500	Y41	✓(3.08)	✓(3.50)	✓(2.87)	✓(3.04)	✓(3.49)	✓(2.97)	✓(2.82)
s-s	N501	Y41	✓(3.23)	X	X(p)	X(p)	X(p)	X(p)	X(p)
s-s	Q498	X38	✓(2.92)	X	X	X	✓(3.02)	X	X
s-s	N501	K353	X(p)	✓(3.36)	X(p)	X(p)	X(p)	✓(3.30)	✓(3.16)
s-s	Y449	X38	✓(2.92)	X	X	X	✓(2.65)	X	X
s-s	Y449	Q42	✓(3.03)	X	✓(2.99)	X	✓(2.91)	X	X(p)
SB	ACE2	ACE2	D38	I38	S38	T38	E38	K38	W38
	K353	X38	✓(3.66)	X	X	X	✓(3.71)	X	X
HB	ACE2	ACE2	D38	I38	S38	T38	E38	K38	W38
b-s	Q42	X38	✓(3.04)	X	✓(3.41)	X	X(p)	X(p)	X
HB	COV-2	COV-2	D38	I38	S38	T38	E38	K38	W38
s-s	N501	Q498	✓(3.02)	✓(3.06)	✓(3.01)	✓(2.45)	✓(3.31)	X	X
s-s	Y449	Q498	✓(3.04)	X	✓(3.48)	X	✓(2.90)	X	X(p)
CI	COV-2	ACE2	D38	I38	S38	T38	E38	K38	W38
vdW/h	Q498	Y41	✓	✓	✓	✓(p)	✓	✓(p)	X
p	Q498	Q42	✓	X	X	X	✓	X	X

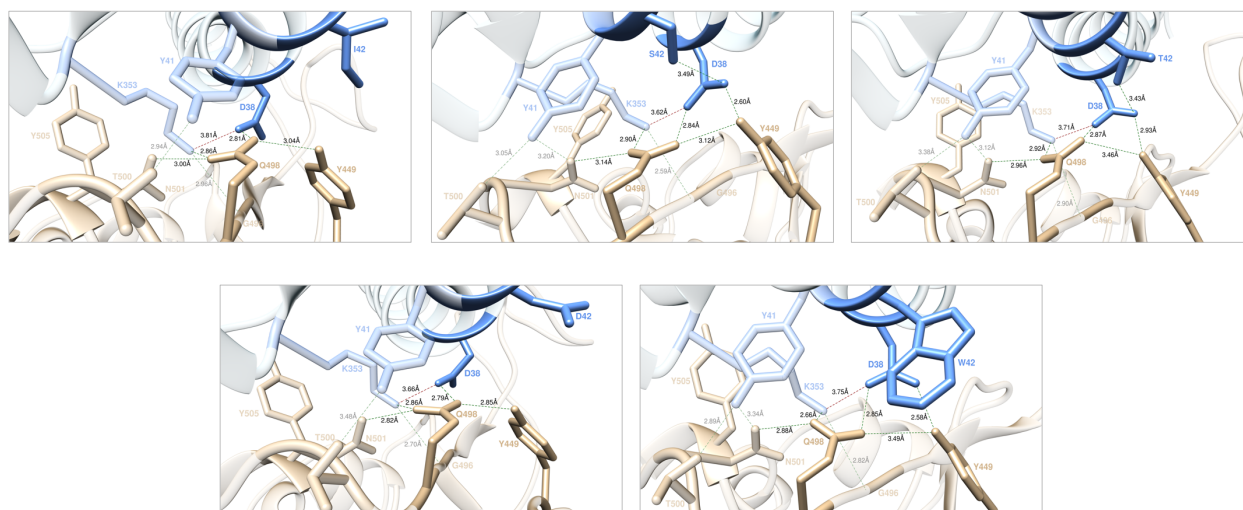


Figure S13. Main interactions involving the ACE2 I42 (top left), S42 (top middle), T42 (top right), D42 (bottom left), and W42 (bottom right) at the interface with S-RBD_{CoV-2} as obtained from the corresponding equilibrated MD simulations. The wild-type Q42 and the K42 mutant are presented and discussed in the main text (Figure 10A-B). Colors and other explanations as in Figure S1. For further details see Tables S1 and S15.

Table S15. Main intermolecular and intramolecular interactions between the wild-type ACE2 residue Q42 and all considered mutants* at the protein-protein interface detected during MD simulations of ACE2 in complex with the RBD of SARS-CoV-2 (CoV-2). Acronyms and other explanations as in Table S3. *Mutant K42 is discussed in detail in main text.

HB	COV-2	ACE2	Q42	I42	S42	T42	D42	K42	W42
s-s	Q498	K353	✓(2.87)	✓(2.86)	✓(2.90)	✓(2.92)	✓(2.86)	✓(2.70)	✓(2.66)
b-s	G496	K353	✓(2.95)	✓(2.96)	✓(2.59)	✓(2.90)	✓(2.70)	✓(2.84)	✓(2.82)
s-s	T500	Y41	✓(3.08)	✓(2.94)	✓(3.05)	✓(3.38)	✓(3.48)	✓(3.12)	✓(2.89)
s-s	N501	Y41	✓(3.23)	✗(p)	✓(3.20)	✓(3.12)	✗(p)	✓(3.37)	✓(3.34)
s-s	Q498	D38	✓(2.92)	✓(2.81)	✓(2.84)	✓(2.87)	✓(2.79)	✓(2.91)	✓(2.85)
s-s	Y449	D38	✓(2.92)	✗	✓(2.60)	✓(2.93)	✗	✓(3.26)	✓(2.58)
s-s	Y449	X42	✓(3.03)	✗	✗(p)	✗(p)	✗	✓(2.43)	✗
SB	ACE2	ACE2	Q42	I42	S42	T42	D42	K42	W42
	K353	D38	✓(3.66)	✓(3.81)	✓(3.62)	✓(3.71)	✓(3.66)	✓(3.73)	✓(3.75)
b-s	D38	X42	✓(3.04)	✗	✓(s-s,3.49)	✓(s-s,3.43)	✗	✓(SB,3.91)	✗
HB	COV-2	COV-2	Q42	I42	S42	T42	D42	K42	W42
s-s	N501	Q498	✓(3.02)	✓(3.00)	✓(3.14)	✓(2.96)	✓(2.82)	✓(2.98)	✓(2.88)
s-s	Y449	Q498	✓(3.04)	✓(3.04)	✓(3.12)	✓(3.46)	✓(2.85)	✓(3.20)	✓(3.49)
CI	COV-2	ACE2	Q42	I42	S42	T42	D42	K42	W42
p	N501	K353	✓	✓	✓	✓	✓	✓	✓
vdW/h	Q498	Y41	✓	✓(p)	✓	✓	✓(p)	✓	✓
p	Q498	X42	✓	✗	✓	✓	✗	✓	✗

The qualitative *in silico*/experimental data comparison reported in Figure 11C (main text) for the mutagenesis of ACE Q42 into I42 shows that a stabilizing effect is reported by experiment⁴ while an interface disrupting effect is anticipated *in silico* ($\Delta\Delta G_{ACE2}(Q42I) = -2.46 \pm 0.10$ kcal/mol, Table S1). The analysis of the corresponding MD trajectory for the ACE2 I42 mutant in complex with the S-RBD_{CoV-2} (Figure S13 (top left) and Table S15) reveals that, with respect to the wild-

type assembly, several important inter- and intramolecular interactions are no longer established in the presence of this mutant residue, that is: i) the three intermolecular HBs between the viral Y449 and ACE2 D38 and I42, and between the viral N501 and ACE2 Y41, respectively; ii) the internal HB between D38 and I42; and iii) the intermolecular CI with the viral N498. Also, the experimental results contextually show a slightly positive effect for valine while the opposite results for alanine (in agreement with our previous findings).³ Accordingly, we retain that a polar-to-hydrophobic substitution at this receptor position ultimately exerts a mildly destabilizing effect on the relevant ACE2/S-RBD_{CoV-2} complex formation.

Moreover, as it can be seen comparing the image for the wild-type Q42 (Figure 10A in main text) and those for the S42 and T42 mutants (Figure S13, top middle and right panel, respectively), according to the present MD simulations these three ACE2 residues can engage the same type and number of intra- and intermolecular interactions at the corresponding receptor/S-RBD_{CoV-2} interface. Thus, for both S42 and T42 a neutral effect is predicted ($\Delta\Delta G_{ACE2}(Q42S) = -0.08 \pm 0.06$ kcal/mol and $\Delta\Delta G_{ACE2}(Q42T) = +0.10 \pm 0.11$ kcal/mol, respectively, Figure 11C in main text and Table S1). Interestingly, *in silico* and *in vitro* data do coincide for the T42 mutant while experiment reveals a slightly interface disrupting behavior for the S42 ACE2 isoform⁴ (Figure 11C). Given the uncertainty underlying both computational and experimental techniques, the arbitrariness in the quantification range of stabilizing/destabilizing effects, and the MD-based evidence supporting the fact S42 and T42 can form the same interface interactions, we retain that these two alternative residues are both equivalent to the wild-type ACE2 Q42 and, as such, have a neutral effect on the relative protein/protein interface.

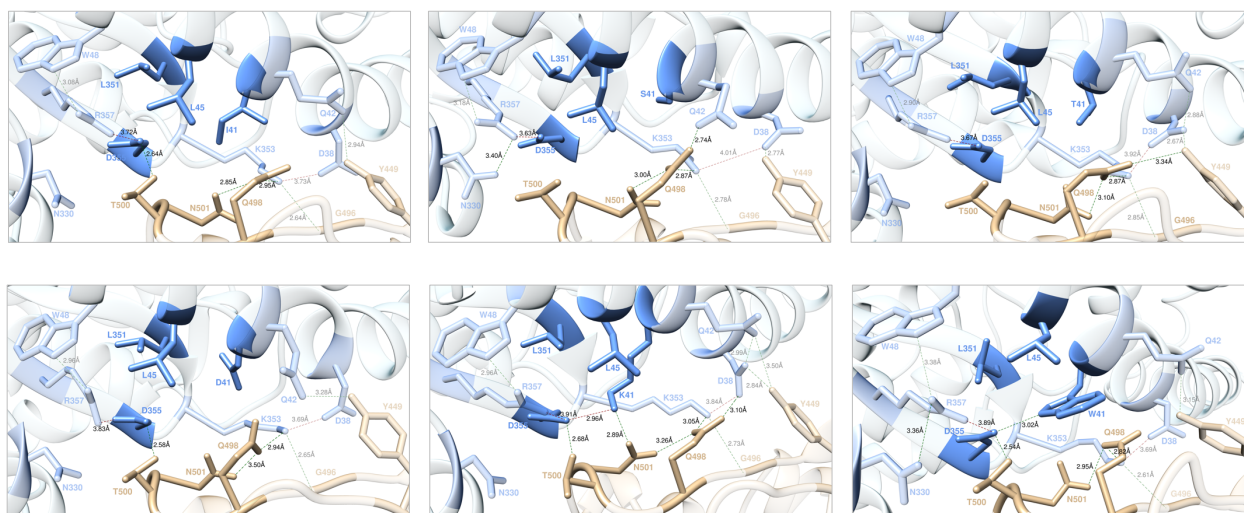


Figure S14. Main interactions involving the ACE2 I41 (top left), S41 (top middle), T41 (top right), D41 (bottom left), K41 (bottom middle) and W41 (bottom right) at the interface with S-RBD_{CoV-2} as obtained from the corresponding equilibrated MD simulations. The wild-type Y41 is presented and discussed in the main text (Figure 12A). Colors and other explanations as in Figure S1. For further details see Tables S1 and S16.

Table S16. Main intermolecular and intramolecular interactions between the wild-type ACE2 residue Y41 and all considered mutants at the protein-protein interface detected during MD simulations of ACE2 in complex with the RBD of SARS-CoV-2 (COV-2). Acronyms and other explanations as in Table S3.

HB	COV-2	ACE2	Y41	I41	S41	T41	D41	K41	W41
s-s	T500	X41	✓(3.08)	✗	✗	✗	✗	✗	✗
s-s	N501	X41	✓(3.23)	✗	✗	✗	✗	✓(2.89)	✗
s-s	T500	D355	✓(2.77)	✓(2.64)	✗(p)	✗(p)	✓(2.58)	✓(2.68)	✓(2.54)
s-s	Q498	K353	✓(2.87)	✓(2.95)	✓(2.87)	✓(2.87)	✓(2.94)	✓(3.05)	✓(2.82)
b-s	G496	K353	✓(2.95)	✓(2.64)	✓(2.78)	✓(2.85)	✓(2.65)	✓(2.73)	✓(2.61)
s-s	Q498	D38	✓(2.92)	✗(p)	✗	✗(p)	✗	✓(3.10)	✗(p)
s-s	Y449	D38	✓(2.92)	✗	✓(2.77)	✓(2.67)	✗(p)	✓(2.84)	✗(p)
s-s	Y449	Q42	✓(3.03)	✓(2.94)	✗(p)	✗(p)	✓(3.28)	✓(3.50)	✓(3.15)
SB	ACE2	ACE2	Y41	I41	S41	T41	D41	K41	W41
	R357	D355	✓(3.68)	✓(3.72)	✓(3.63)	✓(3.67)	✓(3.83)	✓(3.91)	✓(3.89)
	K353	D38	✓(3.66)	✓(3.73)	✓(4.01)	✓(3.92)	✓(3.69)	✓(3.84)	✓(3.69)
HB	ACE2	ACE2	Y41	I41	S41	T41	D41	K41	W41
s-s	D355	X41	✓(2.78)	✗	✗	✗	✗	✓(2.96)	✓(3.02)
b-s	D38	Q42	✓(3.04)	✗	✗(p)	✓(s-s,2.88)	✗(p)	✓(s-s,2.99)	✗
s-s	W48	R357	✓(2.61)	✓(3.08)	✓(3.18)	✓(2.90)	✓(2.96)	✓(2.96)	✓(3.38)
HB	COV-2	COV-2	Y41	I41	S41	T41	D41	K41	W41
s-s	N501	Q498	✓(3.02)	✓(2.85)	✓(3.00)	✓(3.10)	✓(3.50)	✓(3.26)	✓(2.95)
s-s	Y449	Q498	✓(3.04)	✗(p)	✗(p)	✓(3.34)	✗	✗(p)	✗(p)
CI	COV-2	ACE2	Y41	I41	S41	T41	D41	K41	W41
vdW/h	Q498	X41	✓	✓	✗	✓	✓	✓	✓
p	N501	K353	✓	✓	✓	✓	✓	✓	✓

p	Q498	Q42	✓	✗	✓(HB,2.74)	✗	✓	✗	✗
p	T500	R357	✓	✓	✓	✓	✓	✗	✓
vdw/h	T500	N330	✓	✓	✓	✓	✓	✓	✓
CI	ACE2	ACE2	Y41	I41	S41	T41	D41	K41	W41
vdW/h	K353	X41	✓	✓	✗	✓	✓	✓	✓
vdW/h	L45	X41	✓	✓	✗	✓	✓	✓	✓
vdW/h	L351	X41	✓	✗	✗	✗	✗	✓	✓
vdW/h	L351	R357	✓	✓	✓	✓	✓	✓	✓
vdW/h	N330	R357	✓	✓	✓(HB,3.40)	✗	✓	✓	✓(HB,3.36)

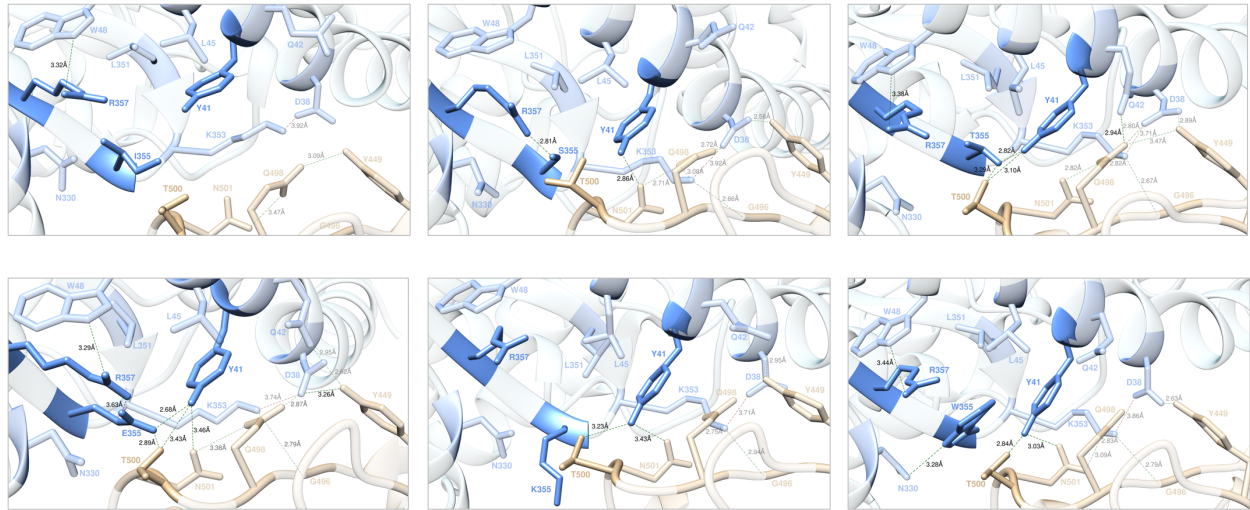


Figure S15. Main interactions involving the ACE2 I355 (top left), S355 (top middle), T355 (top right), E355 (bottom left), K355 (bottom middle) and W355 (bottom right) at the interface with S-RBD_{CoV-2} as obtained from the corresponding equilibrated MD simulations. The wild-type D355 is presented and discussed in the main text (Figure 12A). Colors and other explanations as in Figure S1. For further details see Tables S1 and S17.

Table S17. Main intermolecular and intramolecular interactions between the wild-type ACE2 residue D355 and all considered mutants at the protein-protein interface detected during MD simulations of ACE2 in complex with the RBD of SARS-CoV-2 (COV-2). Acronyms and other explanations as in Table S3.

HB	COV-2	ACE2	D355	I355	S355	T355	E355	K355	W355
s-s	T500	Y41	✓(3.08)	✗	✗	✓(3.10)	✓(3.43)	✓(3.23)	✓(2.84)
s-s	N501	Y41	✓(3.23)	✗	✓(2.86)	✗	✓(3.46)	✓(3.43)	✓(3.03)
s-s	T500	X355	✓(2.77)	✗	✗(p)	✓(3.29)	✓(2.89)	✗	✗
s-s	Q498	K353	✓(2.87)	✗(p)	✓(3.08)	✓(2.82)	✗(p)	✓(2.75)	✓(2.83)
b-s	G496	K353	✓(2.95)	✗	✓(2.66)	✓(2.67)	✓(2.79)	✓(2.94)	✓(2.79)
s-s	Q498	D38	✓(2.92)	✗(p)	✓(2.72)	✓(2.80)	✓(2.87)	✗(p)	✗(p)
s-s	Y449	D38	✓(2.92)	✗(p)	✓(2.58)	✓(2.89)	✓(3.26, 2.62)	✗(p)	✓(2.63)
s-s	Y449	Q42	✓(3.03)	✗	✗	✗(p)	✗(p)	✓(2.95)	✗
SB	ACE2	ACE2	D355	I355	S355	T355	E355	K355	W355
	R357	X355	✓(3.68)	✗	✓(HB, 2.81)	✗	✓(3.63)	✗	✗
	K353	D38	✓(3.66)	✓(3.92)	✓(3.92)	✓(3.71)	✓(3.74)	✓(3.71)	✓(3.86)
HB	ACE2	ACE2	D355	I355	S355	T355	E355	K355	W355
s-s	Y41	X355	✓(2.78)	✗	✗	✓(2.82)	✓(2.68)	✗	✗
b-s	D38	Q42	✓(3.04)	✗	✗	✗(p)	✓(2.95)	✗	✗
s-s	W48	R357	✓(2.61)	✓(3.32)	✗(p)	✓(3.38)	✓(3.29)	✗	✓(3.44)
s-s	N330	X355	✗	✗	✗	✗	✗	✗	✓(3.28)
HB	COV-2	COV-2	D355	I355	S355	T355	E355	K355	W355
s-s	N501	Q498	✓(3.02)	✓(3.47)	✓(2.71)	✓(2.82)	✓(3.38)	✗(p)	✓(3.09)
s-s	Y449	Q498	✓(3.04)	✓(3.09)	✗(p)	✓(3.47)	✗(p)	✗(p)	✗(p)
CI	COV-2	ACE2	D355	I355	S355	T355	E355	K355	W355
vdW/h	Q498	Y41	✓	✗	✓	✓	✓	✓	✓

p	N501	K353	✓	✗	✓	✓	✓	✗	✓
p	Q498	Q42	✓	✗	✗	✓(HB,2.94)	✓	✓	✗
p	T500	R357	✓	✗	✓	✗	✓	✗	✗
vdw/h	T500	N330	✓	✗	✗	✓	✓	✓	✓
CI	ACE2	ACE2	D355	I355	S355	T355	E355	K355	W355
vdW/h	L351	R357	✓	✓	✓	✗	✓	✓	✓
vdW/h	N330	R357	✓	✓(p)	✓	✓	✓	✗	✗

At variance with experiment⁴ for which a negative effect is foreseen for the ACE2 D355E mutation (Figure 13B, main text), our calculations predict a neutral effect corresponding to a $\Delta\Delta G_{ACE2}(D355E)$ value of -0.06 ± 0.11 kcal/mol (Table S1). In line with this, the inspection of the bottom left panel in Figure S15 and the list of interactions reported in Table S17 reveals that all main intermolecular contacts across the protein-protein binding interface seen in the wild-type complex are preserved, the double HB between D38 and Y449 in the mutant isoform compensating for the weaker polar interaction between the receptor K353 and the viral protein Q498. Accordingly, we retain that the conservative D355E substitution has no significant effect on the affinity of the mutant ACE2 for the receptor binding domain of the viral S-protein.

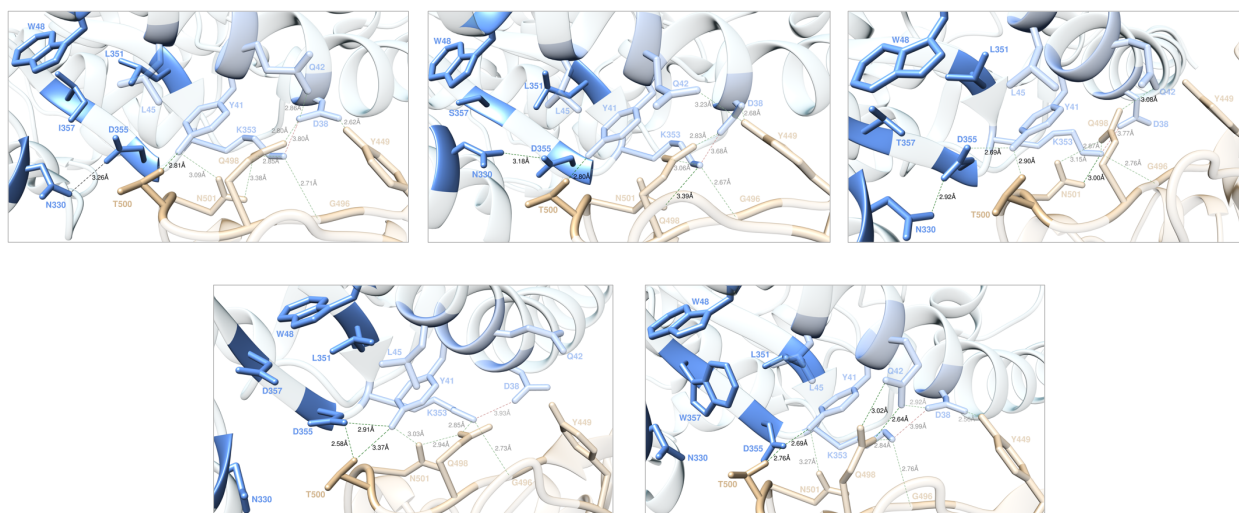


Figure S16. Main interactions involving the ACE2 I357 (top left), S357 (top middle), T357 (top right), D357 (bottom left), and W357 (bottom right) at the interface with S-RBD_{CoV-2} as obtained from the corresponding equilibrated MD simulations. The wild-type R357 and the K357 mutant are presented and discussed in the main text (Figure 12A-B). Colors and other explanations as in Figure S1. For further details see Tables S1 and S18.

Table S18. Main intermolecular and intramolecular interactions between the wild-type ACE2 residue R357 and all considered mutants* at the protein-protein interface detected during MD simulations of ACE2 in complex with the RBD of SARS-CoV-2 (COV-2). Acronyms and other explanations as in Table S3. *Mutant K357 is discussed in detail in main text.

HB	COV-2	ACE2	R357	I357	S357	T357	D357	K357	W357
s-s	T500	Y41	✓(3.08)	✓(2.81)	✓(2.80)	✓(2.90)	✓(3.37)	✓(3.36)	✗
s-s	N501	Y41	✓(3.23)	✓(3.09)	✗(p)	✗(p)	✓(3.03)	✓(2.81)	✓(3.27)
s-s	T500	D355	✓(2.77)	✗(p)	✗(p)	✗	✓(2.58)	✓(2.73)	✓(2.76)
s-s	Q498	K353	✓(2.87)	✓(2.85)	✓(3.06)	✓(2.87)	✓(2.85)	✓(2.71)	✓(2.84)
b-s	G496	K353	✓(2.95)	✓(2.71)	✓(2.67)	✓(2.76)	✓(2.73)	✓(2.80)	✓(2.76)
s-s	Q498	D38	✓(2.92)	✓(2.80)	✓(2.83)	✗(p)	✗(p)	✓(3.37)	✗(p)
s-s	Y449	D38	✓(2.92)	✓(2.62)	✓(2.68)	✗(p)	✗(p)	✓(3.10)	✓(2.56)
s-s	Y449	Q42	✓(3.03)	✗(p)	✓(3.23)	✗(p)	✗(p)	✓(2.98)	✗
SB	ACE2	ACE2	R357	I357	S357	T357	D357	K357	W357
	D355	X357	✓(3.68)	✗	✗	✗	✗	✓(3.63,3.77)	✗
	K353	D38	✓(3.66)	✓(3.80)	✓(3.68)	✓(3.77)	✓(3.93)	✓(3.82)	✓(3.99)
HB	ACE2	ACE2	R357	I357	S357	T357	D357	K357	W357
s-s	Y41	D355	✓(2.78)	✗	✗(p)	✓(2.69)	✓(2.91)	✓(2.89)	✓(2.69)
b-s	D38	Q42	✓(3.04)	✓(s-s,2.86)	✗(p)	✗(p)	✗(p)	✓(s-s,2.90)	✓(s-s,2.92)
s-s	W48	X357	✓(2.61)	✗	✗(p)	✗	✗	✗(p)	✗(π/π)
s-s	N330	D355	✗	✓(3.26)	✓(3.18)	✓(2.92)	✗	✗	✗
HB	COV-2	COV-2	R357	I357	S357	T357	D357	K357	W357
s-s	N501	Q498	✓(3.02)	✓(3.38)	✗(p)	✓(3.15)	✓(2.94)	✗(p)	✗
s-s	Y449	Q498	✓(3.04)	✗(p)	✗(p)	✗(p)	✗(p)	✓(3.40)	✗
CI	COV-2	ACE2	R357	I357	S357	T357	D357	K357	W357
vdW/h	Q498	Y41	✓	✓	✓	✓	✓	✓	✓

p	N501	K353	✓	✓	✓(HB,3.39)	✓(HB,3.00)	✓	✗	✓
p	Q498	Q42	✓	✓	✓	✓(HB,3.08)	✓	✓	✓(HB,2.64,3.02)
p	T500	X357	✓	✗	✗	✗	✗	✓	✗
vdw/h	T500	N330	✓	✓	✓	✓	✗	✓	✓
CI	ACE2	ACE2	R357	I357	S357	T357	D357	K357	W357
vdW/h	L351	X357	✓	✗	✗	✗	✗	✓	✓
vdW/h	N330	X357	✓	✗	✓	✓	✗	✗	✓

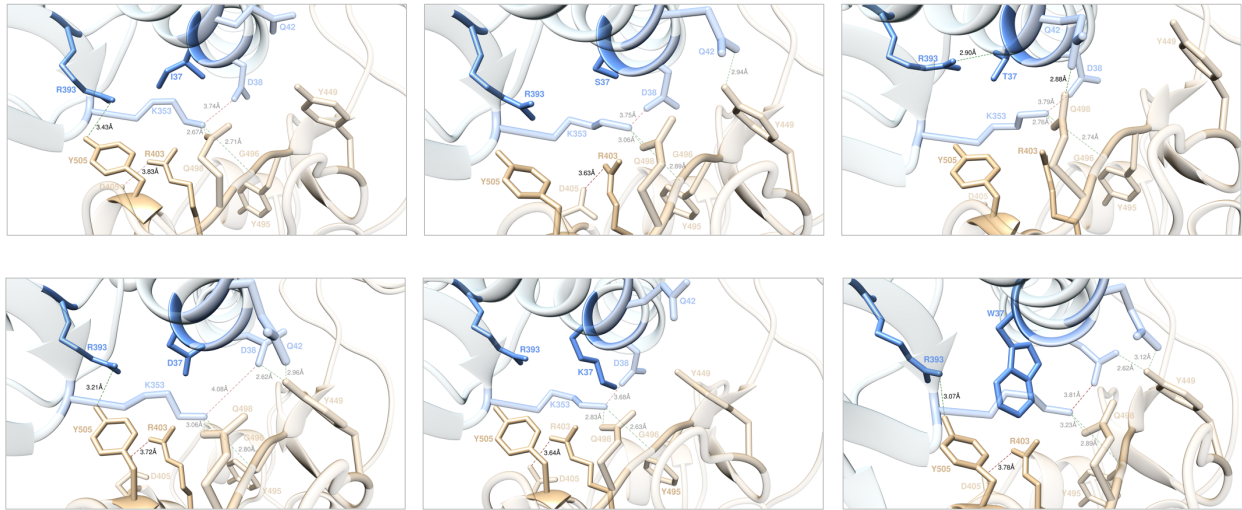


Figure S17. Main interactions involving the ACE2 I37 (top left), S37 (top middle), T37 (top right), D37 (bottom left), K37 (bottom middle) and W37 (bottom right) at the interface with S-RBD_{CoV-2} as obtained from the corresponding equilibrated MD simulations. The wild-type E37 is presented and discussed in the main text (Figure 14A). Colors and other explanations as in Figure S1. For further details see Tables S1 and S19.

Table S19. Main intermolecular and intramolecular interactions between the wild-type ACE2 residue E37 and all considered mutants at the protein-protein interface detected during MD simulations of ACE2 in complex with the RBD of SARS-CoV-2 (COV-2). Acronyms and other explanations as in Table S3.

HB	COV-2	ACE2	E37	I37	S37	T37	D37	K37	W37
s-s	Y505	X37	✓(3.15)	X	X	X	X	X	X
s-s	Q498	K353	✓(2.87)	✓(2.67)	✓(3.06)	✓(2.76)	✓(3.06)	✓(2.83)	✓(3.23)
b-s	G496	K353	✓(2.95)	✓(2.71)	✓(2.89)	✓(2.74)	✓(2.80)	✓(2.63)	✓(2.89)
s-s	Q498	D38	✓(2.92)	X(p)	X(p)	X(p)	X(p)	X(p)	X(p)
s-s	Y449	D38	✓(2.92)	X	X	X	✓(2.62)	X	✓(2.62)
s-s	Y449	Q42	✓(3.03)	X	✓(2.94)	X	✓(2.96)	X	✓(3.12)
SB	COV2	ACE2	E37	I37	S37	T37	D37	K37	W37
	R403	X37	✓(3.62)	X	X	X	X	X	X
SB	ACE2	ACE2	E37	I37	S37	T37	D37	K37	W37
	R393	X37	✓(3.93,3.63)	X	X	X(HB,2.90)	X	X	X
	K353	D38	✓(3.66)	✓(3.74)	✓(3.75)	✓(3.79)	✓(4.08)	✓(3.68)	✓(3.81)
SB	COV2	COV2	E37	I37	S37	T37	D37	K37	W37
	D405	R403	✓(3.95)	✓(3.83)	✓(3.63)	X	✓(3.72)	✓(3.64)	✓(3.78)
HB	ACE2	ACE2	E37	I37	S37	T37	D37	K37	W37
b-s	D38	Q42	✓(3.04)	X	X	X(p)	X(p)	X	X(p)
HB	COV-2	COV-2	E37	I37	S37	T37	D37	K37	W37
s-s	Y449	Q498	✓(3.04)	X	X	X	X(p)	X(p)	X(p)
CI	COV-2	ACE2	E37	I37	S37	T37	D37	K37	W37
p	Y505	R393	✓	✓(HB,3.43)	X	X	✓(HB,3.21)	X	✓(HB,3.07)
p	Q498	Q42	✓	X	X	✓(HB,2.88)	✓	X	✓
CI	COV2	COV2	E37	I37	S37	T37	D37	K37	W37
π/c	Y505	R403	✓	X	X	X	✓	✓	X

vdW/h	Y495	R403	✓	✓	✓	✓	✓	✗	✓
-------	------	------	---	---	---	---	---	---	---

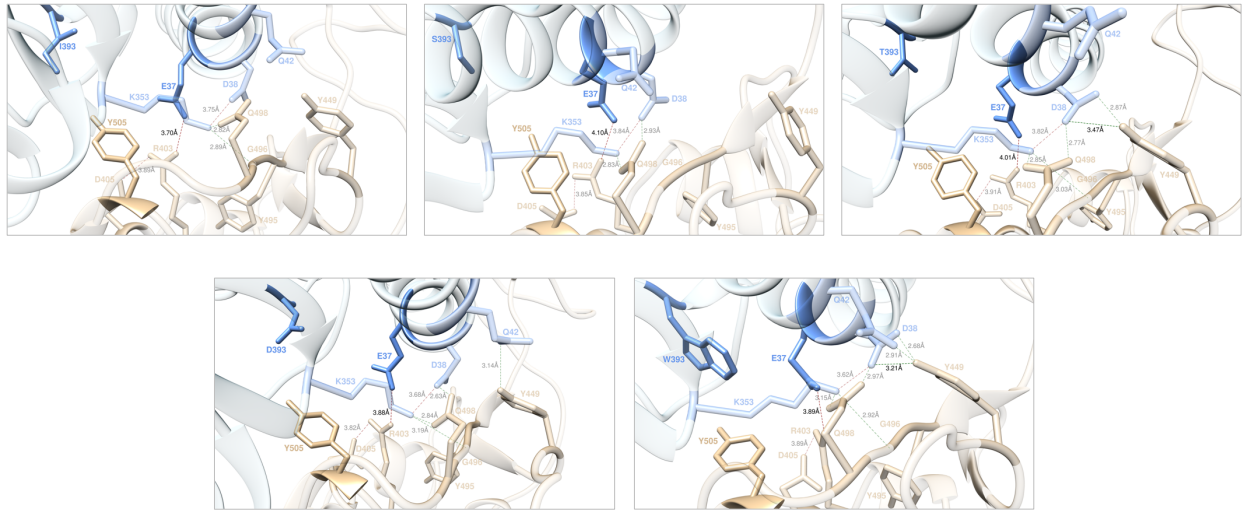


Figure S18. Main interactions involving the ACE2 I393 (top left), S393 (top middle), T393 (top right), D393 (bottom left), and W393 (bottom right) at the interface with S-RBD_{CoV-2} as obtained from the corresponding equilibrated MD simulations. The wild-type R393 and the R393K mutant are presented and discussed in the main text (Figure 14A-B). Colors and other explanations as in Figure S1. For further details see Tables S1 and S20.

Table S20. Main intermolecular and intramolecular interactions between the wild-type ACE2 residue R393 and all considered mutants* at the protein-protein interface detected during MD simulations of ACE2 in complex with the RBD of SARS-CoV-2 (COV-2). Acronyms and other explanations as in Table S3. *Mutant K393 is discussed in detail in main text.

HB	COV-2	ACE2	R393	I393	S393	T393	D393	K393	W393
s-s	Y505	E37	✓(3.15)	✗	✗	✗	✗	✓(2.84)	✗
s-s	Q498	K353	✓(2.87)	✓(2.82)	✓(2.83)	✓(2.85)	✓(2.84)	✓(2.75)	✓(3.15)
b-s	G496	K353	✓(2.95)	✓(2.89)	✗	✓(3.03)	✓(3.19)	✓(2.78)	✓(2.92)
s-s	Q498	D38	✓(2.92)	✗(p)	✓(2.93)	✓(2.77)	✓(2.63)	✓(2.77)	✓(2.97)
s-s	Y449	D38	✓(2.92)	✗	✗	✓(2.87,3.47)	✗	✓(2.83)	✓(2.68,3.21)
s-s	Y449	Q42	✓(3.03)	✗(p)	✗	✗	✓(3.14)	✓(3.17)	✓(2.91)
SB	COV2	ACE2	R393	I393	S393	T393	D393	K393	W393
	R403	E37	✓(3.62)	✓(3.70)	✓(4.10)	✓(4.01)	✓(3.88)	✓(3.84)	✓(3.89)
SB	ACE2	ACE2	R393	I393	S393	T393	D393	K393	W393
	E37	X393	✓(3.93,3.63)	✗	✗	✗	✗	✓(3.73)	✗
	K353	D38	✓(3.66)	✓(3.75)	✓(3.75)	✓(3.82)	✓(3.68)	✓(3.63)	✓(3.62)
SB	COV2	COV2	R393	I393	S393	T393	D393	K393	W393
	D405	R403	✓(3.95)	✓(3.89)	✓(3.84)	✓(3.91)	✓(3.82)	✓(3.74)	✓(3.89)
HB	ACE2	ACE2	R393	I393	S393	T393	D393	K393	W393
b-s	D38	Q42	✓(3.04)	✗	✗(p)	✗	✗	✓(s-s,2.80)	✗(p)
HB	COV-2	COV-2	R393	I393	S393	T393	D393	K393	W393
s-s	Y449	Q498	✓(3.04)	✗	✗	✗	✗	✓(3.29)	✗(p)
CI	COV-2	ACE2	R393	I393	S393	T393	D393	K393	W393
p	Y505	X393	✓	✗	✗	✗	✗	✓(HB,2.84)	✗
p	Q498	Q42	✓	✗(p)	✗	✗	✗	✗	✓
CI	COV2	COV2	R393	I393	S393	T393	D393	K393	W393

π/c	Y505	R403	✓	✓	✓	✓	✗	✓	✗
vdW/h	Y495	R403	✓	✓	✓	✗	✓	✓	✓

According to our calculations, when the ACE2 wild-type R393 is replaced by a threonine, a moderate destabilizing effect at the corresponding protein/protein binding interface is observed ($\Delta\Delta G_{ACE2}(R393T) = -1.98 \pm 0.08$ kcal/mol, Figure 15B in main text and Table S1), whilst a neutral effect is experimentally reported.⁴ As seen from the interaction list in Table S20, the T393 mutant receptor fails to engage the side chains of the two S-RBD_{CoV-2} residues Y505 and Y449 in the two intermolecular HBs with ACE2 E37 and Q42 seen in the wild-type complex, respectively, alongside with some missing inter- and intramolecular CIs (Figures 14A and S18 (top right panel)).

References

1. Shang, J.; Ye, G.; Shi, K.; Wan, Y.; Luo, C.; Aihara, H.; Geng, Q.; Auerbach, A.; Li, F., Structural Basis of Receptor Recognition by SARS-CoV-2. *Nature* **2020**, *581*, 221-224.
2. Lan, J.; Ge, J.; Yu, J.; Shan, S.; Zhou, H.; Fan, S.; Zhang, Q.; Shi, X.; Wang, Q.; Zhang, L.; Wang, X., Structure of the SARS-CoV-2 Spike Receptor-Binding Domain Bound to the ACE2 Receptor. *Nature* **2020**, *581*, 215-220.
3. Laurini, E.; Marson, D.; Aulic, S.; Fermeglia, M.; Pricl, S., Computational Alanine Scanning and Structural Analysis of the SARS-CoV-2 Spike Protein/Angiotensin-Converting Enzyme 2 Complex. *ACS Nano* **2020**, *14*, 11821-11830.
4. Chan, K. K.; Dorosky, D.; Sharma, P.; Abbasi, S. A.; Dye, J. M.; Kranz, D. M.; Herbert, A. S.; Procko, E., Engineering Human ACE2 to Optimize Binding to the Spike Protein of SARS Coronavirus 2. *Science* **2020**, *369*, 1261-1265.